ISSN 1063-7788, Physics of Atomic Nuclei, 2024, Vol. 87, No. 10, pp. 1–8. © Pleiades Publishing, Ltd., 2024.
Russian Text © The Author(s), 00000, published in Yadernaya Fizika i Inzhiniring, 00000, Vol. 00000, No. 00000, pp. 00000–00000.

The Passing of Critical Energy in the Harmonic RF of the U-70 Proton Synchrotron

S. D. Kolokolchikov[a,b,*], Yu. V. Senichev[a,b], and V. A. Kalinin[c]

[a] *Institute of Nuclear Research, Russian Academy of Sciences, Moscow, 117312 Russia*
[b] *Moscow Institute of Physics and Technology, Dolgoprudny, Moscow oblast, 141701 Russia*
[c] *Logunov Institute of High Energy Physics, National Research Center Kurchatov Institute, Protvino, 142281 Russia*
**e-mail: sergey.bell13@gmail.com*

Received January 1, 2024; revised January 1, 2024; accepted January 1, 2024

Abstract—The passing of critical energy at the U-70 proton synchrotron is studied. The stability of motion is ensured by having a jump in critical energy at unvaried values of betatron frequencies. The longitudinal motion is simulated with allowance for higher orders of the coefficient of orbit compaction, along with various impedances and bunch intensities. Experimental data from an accelerator session are presented.

Keywords: critical energy, harmonic high-frequency resonator (RF), longitudinal dynamics, dispersion function modulation

DOI: 10.1134/S106377882410020X

INTRODUCTION

The passing of critical energy is an important problem for the proton beam in the NICA complex now under construction at the Joint Institute of Nuclear Research in Dubna. To study this problem, we investigated the dynamics of longitudinal motion in the vicinity of the critical energy of U-70 at the Institute of High Energy Physics in Protvino.

Raising the rate of passing the critical energy reduces the effects of factors that disturb phase motion. A jump in critical energy is used in many installations at CERN [1] and BNL [2], and is done in the U-70. The critical energy is shifted by distorting the dispersion function with thin quadrupole lenses [3].

Results from this work will help highlight the potential consequences of passing the critical energy and determine the important parameters that affect the dynamics of phase motion.

EQUATIONS OF LONGITUDINAL MOTION

The equations of longitudinal motion describe the evolution of a particle in phase space relative to the reference ~~space~~ [4]:

$$\frac{d\tau}{dt} = \frac{\eta h}{\beta^2 E_0} E, \quad \frac{d\Delta E}{dt} = \frac{Ze}{A}\frac{\omega_0}{2\pi} V \times [\sin(\phi_s - h\omega_0\tau) - \sin\phi_s], \tag{1}$$

where τ is a temporary deviation of the considered particle from the reference particle; β is the relative velocity; $\omega_0 = 2\pi/T_0$ is the angular velocity and corresponding period of revolution; h is the harmonic number; V is the RF amplitude; ϕ_s is the equilibrium particle phase; and the slip factor is $\eta(\delta) = \eta_0 + \eta_1\delta + \cdots$,

$$\eta_0 = \alpha_0 - \frac{1}{\gamma_0^2}, \quad \eta_1 = \frac{3\beta_0^2}{2\gamma_0^2} + \alpha_1 - \alpha_0\eta_0.$$

If the beam energy in Eq. (1) approaches critical value $\gamma \to \gamma_{tr}$, $\eta = \eta_0 \to 0$ and the right-hand side of the equation vanishes. Stability must be ensured when passing the critical energy.

ADIABATICITY AND NONLINEARITY

Far from the critical energy, the frequency of synchrotron oscillations changes weakly over time, and the motion is adiabatic. Near the critical energy, the condition of the adiabaticity of synchrotron motion is violated. The characteristic period of adiabaticity can be estimated by comparing the synchrotron frequency to the rate of change of the holding separatrix (Fig. 1a) [5]:

$$\tau_{\mathrm{ad}} = \left(\frac{\pi\beta^2 mc^2\gamma_{\mathrm{tr}}^4}{\dot{\gamma}\omega_0^2 heV\left|\cos\phi_s\right|}\right)^{1/3}, \tag{2}$$

where γ_{tr} is the Lorentz factor corresponding to the critical energy and $\dot{\gamma}$ is the rate of change in energy. The nonlinearity of longitudinal motion is seen when the characteristic period is comparable to (Fig. 1b)

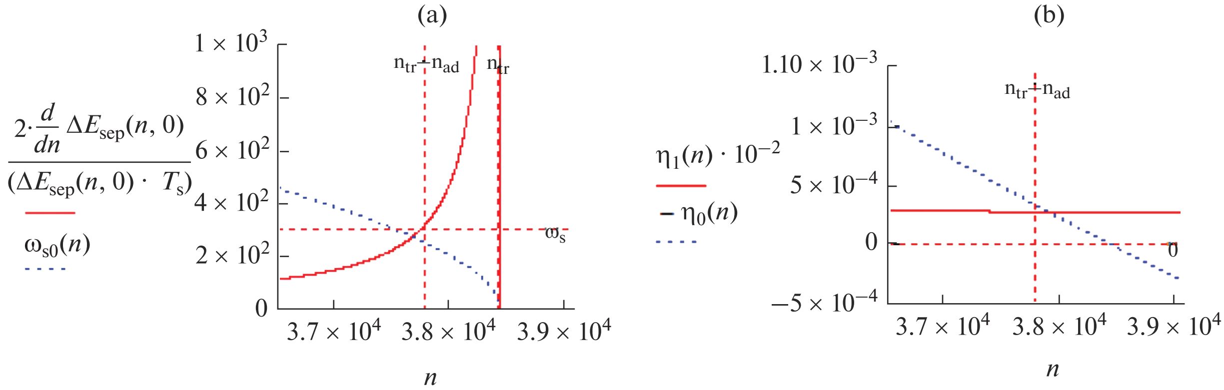

Fig. 1. (a) Classic synchrotron frequency and rate of change of the separatrix envelope in the vicinity of the critical energy as a function of the number of rotations; (b) first- and second-order change in slip factor η_0, $\eta_1\delta$ in the vicinity of the critical energy as a function of the number of revolutions.

$$\tau_{nl} = \frac{\eta_1\hat{\delta}}{\frac{2\dot{\gamma}}{\gamma_{tr}^3}} = \gamma_{tr}\frac{\frac{3}{2}\beta^2+\gamma_{tr}^2\alpha_1}{2\dot{\gamma}}, \tag{3}$$

where $\hat{\delta} \approx 10^{-2}$–$10^{-3}$ is the absolute value of the maximum deviation of the momentum near the critical energy and α_1 is the second order of the coefficient of orbital compaction. It was found in [6] that $\alpha_1 \simeq 0.01$ for the regular FODO structure of the U-70 with natural chromaticity compensated for. Equation (1) also yields the condition for the stability of synchrotron oscillations,

$$\eta_0 \cos\phi_s < 0. \tag{4}$$

It is apparent that the phase of the RF accelerating field must also be shifted when passing the critical energy to obtain longitudinal matching. The estimates for U-70 presented in Table 1 show that adiabatic period (2) can be comparable to nonlinearity period (3): $\tau_{ad} \sim \tau_{nl}$. The longitudinal length of the beam shrinks as the energy approaches the critical value, and the spread of momentum grows. Figure 2 shows results from modeling the passing of critical energy when accelerating particles from 7.0 to 13.0 GeV for $\eta = \eta_0$ and $\eta = \eta_0 + \eta_1\delta$ in different BLonD models [7]. The effect of the second-order slip factor raises the longitudinal emittance.

Table 1. Main parameters of the RF and U-70 ring

Length L, m	1483.699
Coefficient of orbit expansion α_0	0.011120
Coefficient of orbit expansion α_1	0.01
Critical energy, GeV	7.957
Lorentz factor γ_{tr}	7.48
Maximum intensity during the session, ppp (particles per period)	4×10^{12}
Accelerating phase $\sin(\phi_s)$	1/2
Period of diabaticity τ_{ad}, мс	3.218
Period of nonlinearity τ_{nl}, мс	2.646
Harmonic number	30
Accelerating station amplitude, kV	10
Number of accelerating stations	40
Rate of acceleration $\dot{\gamma}$, s^{-1}	42.7

EFFECT OF INDUCTIVE IMPEDANCE

The longitudinal dynamics is also affected by the accelerator elements. Impedance describes the interaction between the beam and elements of the accelerator's structure. Longitudinal impedance $Z_{\parallel}(\omega)$ is especially important when studying the dynamics of passing the critical energy. Analytical calculations of the ring's total impedance are complicated, and we are limited here to its inductive component $Z_n/n = \pm i\times\text{const}$. Negative inductance corresponds to the impedance of the smooth chamber; positive inductance, to the longitudinal impedance of the coupling of pickup electrodes, kicker magnets, and bellows [3].

In our U-70 session, the intensity of a pulse was on the order of $N_{tot} = 4\times10^{12}$ ppp (particles per period). In a bunch, it was on the order of $N_{beam} = 4\times10^{11}$ ppp. Modeling the longitudinal dynamics with energies changing from 7 to 9 GeV showed that the beam remained stable at low intensity $N_{beam} = 4\times10^{11}$ for both negative and positive values of the considered impedance. A strong change in the symmetry of the phase volume and an increase in the longitudinal emittance were observed for high intensities $N_{beam} = 1\times10^{12}$ (Fig. 3, Table 2). According to the experimental data, the initial value of the bunch length was $\tau_L = 4t_\sigma \simeq 20$ ns for $E_0 = 7$ GeV.

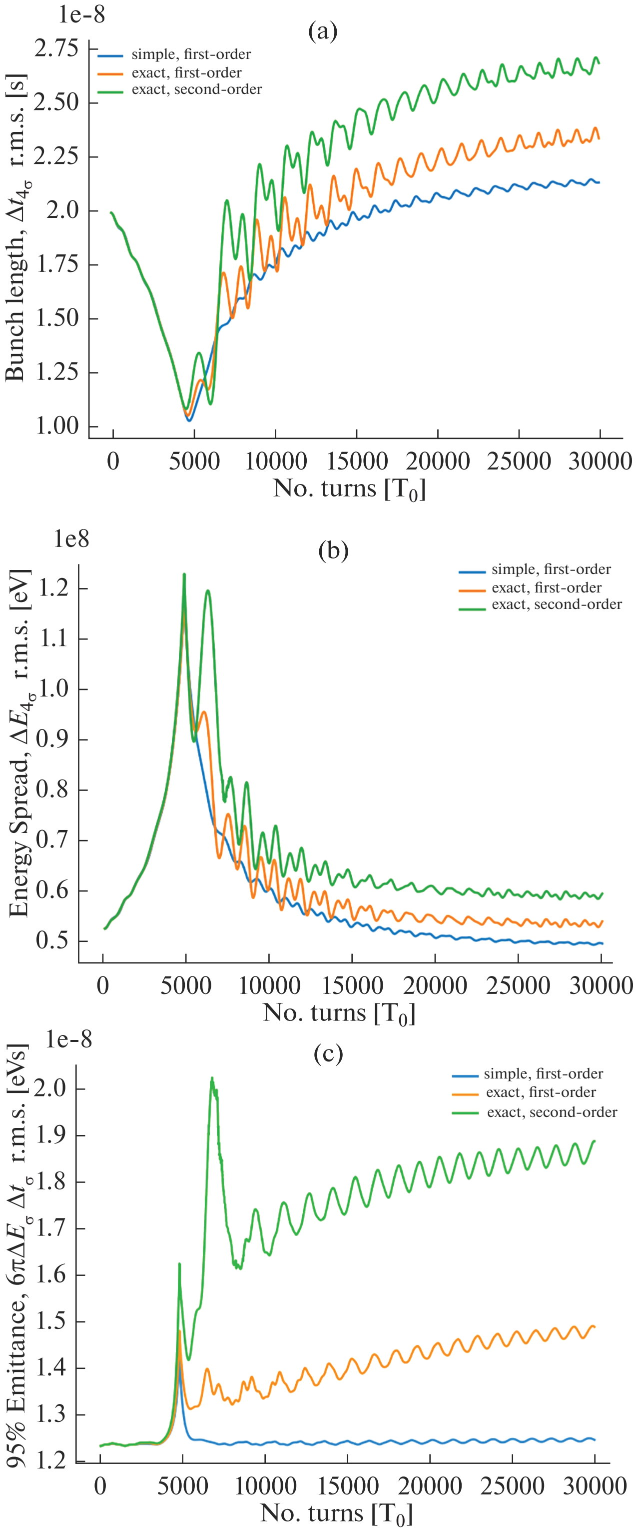

Fig. 2. Dependence of (a) the bunch length, (b) the spread of energy inside the bunch, and (c) the longitudinal emittance on the number of revolutions in the vicinity of the critical energy upon changing it from 7 to 13 GeV for three models without a jump, and allowing for impedance. The blue curve reflects only the first order $\eta = \eta_0$ for a simple solver; orange, only the $\eta = \eta_0$ of an exact solver; and green, only $\eta = \eta_0 + \eta_1\delta$.

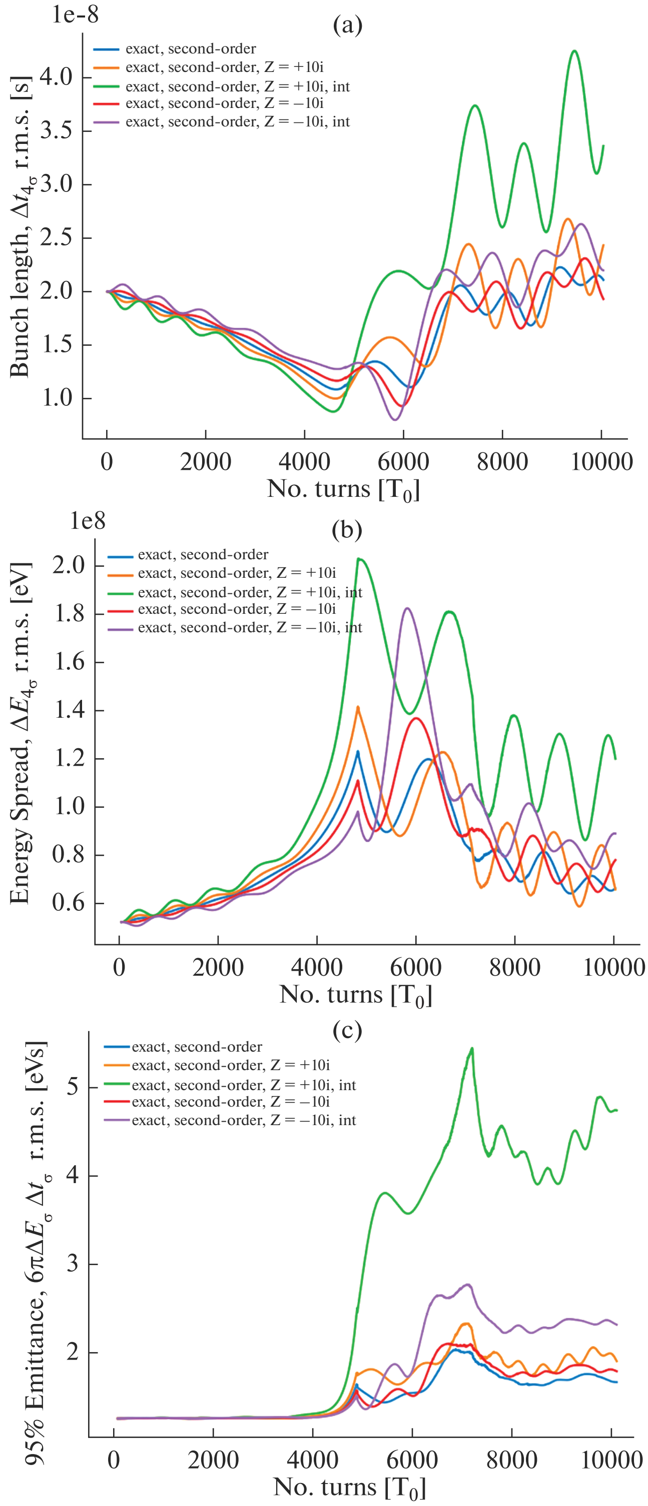

Fig. 3. Dependene of (a) the bunch length, (b) the spread of energy inside the bunch, and (c) the longitudinal emittance on the number of revolutions in the vicinity of the critical energy upon changing the energy from 7 to 9 GeV without a jump, allowing for different types of impedance and intensities.

Table 2. Main parameters of the RF and U-70 ring

Modeling parameters	95% phase volume	Preservation of the beam (9 GeV)	Features
$\alpha_1 = 0$, simple Without impedance	1.23	100%	Simple model Emittance does not increase
$\alpha_1 = 0$, exact Without impedance	1.4	99.65%	Exact model, no MCF nonlinearity, influence of nonadiabaticity, increased emittance
$\alpha_1 = 0.01$, exact Without impedance	1.8	99.65%	Effect of MCF nonlinearity Emittance grows by 1.5 times
$\alpha_1 = 0.01$, exact $Z_n/n = -i10$ 4×10^{11} ppb	1.8	99.65%	Bunch length shrinks after γ_{tr}, focusing after γ_{tr} Increased emittance
$\alpha_1 = 0.01$, exact $Z_n/n = +i10$ 4×10^{11} ppb	1.9	99.60%	Bunch length shrinks after γ_{tr}, wiggling after γ_{tr} Increased emittance
$\alpha_1 = 0.01$, exact $Z_n/n = -i10$ 1×10^{12} ppb	2.3	99.60%	Strong reduction in bunch length before γ_{tr}, increased emittance
$\alpha_1 = 0.01$, exact $Z_n/n = +i10$ 1×10^{12} ppb	4.1	98.60%	Enhanced amplitude of quadrupole oscillations; strong increase in emittance

For a Gaussian distribution, $\Delta E_0 = 4E_\sigma = 52.7$ MeV. $\varepsilon_{095\%} = 1.23$ eV s.

CRITICAL ENERGY JUMP

To maintain stability of longitudinal motion, the longitudinal emittance must not be raised when passing the critical energy. The U-70 therefore uses jumps in critical energy [8]. The rate of passing the critical energy grows, while ~~that of~~ acceleration does not. This is achieved by altering the parameters of the accelerator to change α_0. The coefficient of orbit expansion is generally defined as the integral

$$\alpha = \frac{1}{C}\int_0^C \frac{D(s)}{\rho(s)}ds, \quad (5)$$

where $D(s)$ is the function of dispersion and $\rho(s)$ is the orbital curvature. The coefficient of orbit expansion can be changed by modulating the function of dispersion, since $\rho(s)$ does not changed.

Such modulation in the U-70 synchrotron is done by quadrupoles in the 2nd and 8th blocks of each superperiod [9]. Figure 4 shows the Twiss parameters for one superperiod consisting of 10 magnetic blocks with a combined function for both the regular U-70 structure and a structure with a distorted dispersion function [10]. The quadrupoles positioned at every

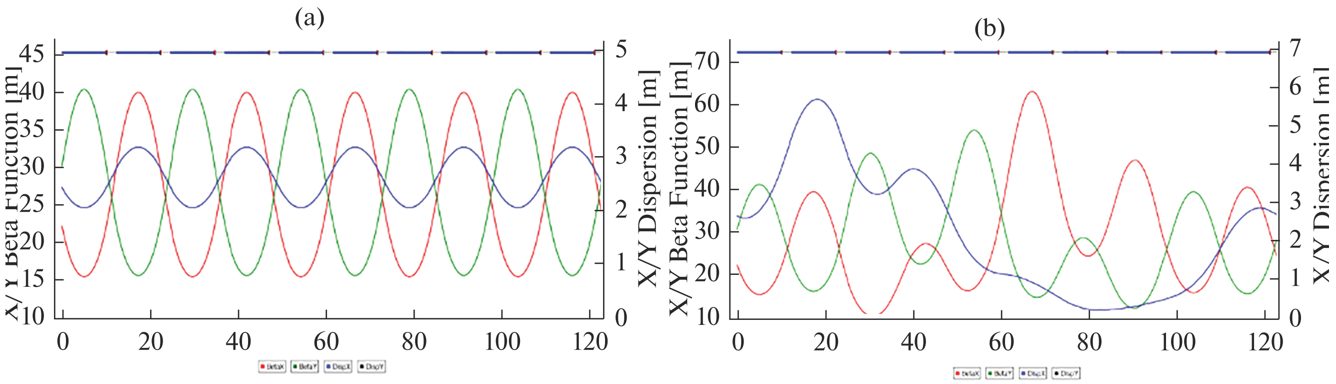

Fig. 4. Twiss parameters β_x, β_y, D_x for the U-70 superperiod: (a) regular structure; (b) structure with modulated dispersion.

Table 3. Main parameters of the RF and U-70 ring

Time after injection, ms	Operating point	Relative to the jump
290	9.921 × 9.842	before the procedure
295	9.917 × 9.808	start of the procedure
310	9.849 × 9.787	middle of the procedure
326	9.780 × 9.771	moment of the jump
330	9.902 × 9.809	after

half period have opposite polarities. There is no shift in the operating point with such dispersion modulation. Table 3 gives the values of the operating point when raising the critical energy and the jump. The critical energy is thus raised at the leading edge by $\Delta\gamma_{tr} = 0.9$ for 36 ms, and the jump itself takes 1ms at the trailing edge. A schematic diagram of the procedure is shown in Fig. 5, along with the corresponding first-order change in the slip factor. The jump procedure at our U-70 session is described in Fig. 6a; the longitudinal linear density of the bunch relative to the RF phase at the moment of the jump is displayed in Fig. 6b.

The data from modeling the longitudinal motion correspond to the change in the bunch length during the acceleration cycle at our U-70 session (Fig. 7). Results from modeling the longitudinal motion (Fig. 8, Table 4) are shown for different models at accelerations of 6.9 to 12.9 GeV [9] for a jump in critical energy and another allowing for impedances of the type $Z_n/n = \pm \times$ const and different intensities of accelera-

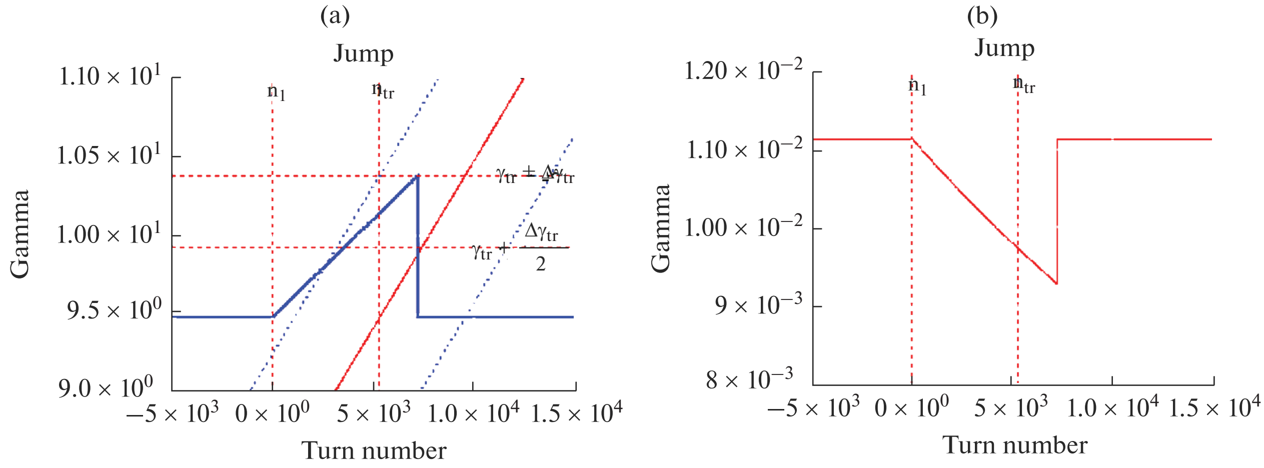

Fig. 5. (a) Increase in critical energy during the jump procedure; (b) corresponding change in the first order of slip factor η_0.

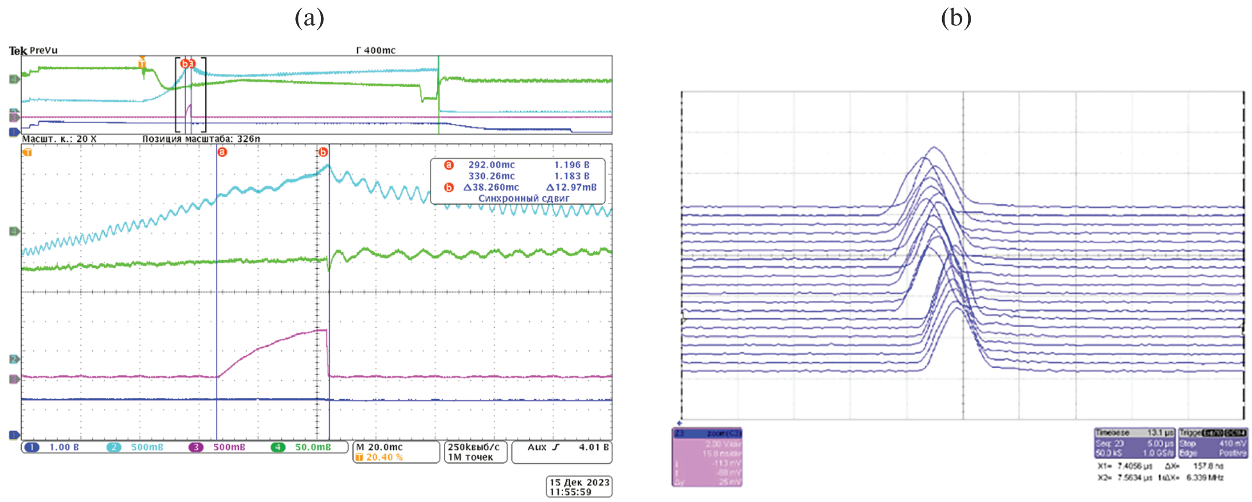

Fig. 6. (a) Jump in critical energy in our U-70 session. The green curve shows the signal from the phase sensor; the violet line is the gradient in the windings of the additional quadrupoles; and the blue line is the signal from the peak detector. (b) Longitudinal linear density of the bunch, relative to the RF phase at the moment of the jump.

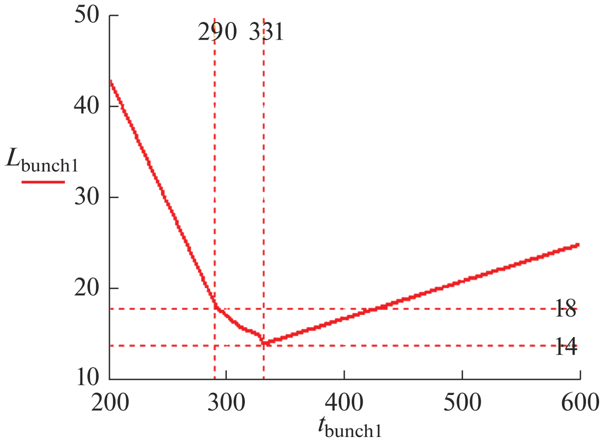

Fig. 7. Change in the bunch length during the acceleration cycle in our U-70 session.

tion from 6.9 to 8.9 GeV (Fig. 9). The initial values are $\tau_L = 4t_\sigma \simeq$ 20 ns at $E_0 = 6.9$ GeV, $\Delta E_0 = 4E_\sigma =$ 49.3 MeV, and $\varepsilon_{095\%} = 1.16$ eV s.

Comparing the two ways of passing the critical energy (with and without a jump in critical energy), we may conclude that the longitudinal length of the bunch was reduced less with a jump. The considered impedances therefore also disturbed the bunch to a lesser extent. An increase in emittance was observed only when considering an intense bunch where the number of particles was $N_{beam} = 1\times10^{12}$ ppb.

CONCLUSIONS

The passing of critical energy in harmonic RF with and without a jump was examined in a session on the U-70 proton synchrotron. The longitudinal dynamics were modeled numerically for different impedances and intensities of bunches. It was shown that the rate of acceleration plays a key role in the passing of critical energy. A jump in critical energy was used to increase it. The critical energy was changed by modulating the dispersion function, allowing us to control the longitudinal emittance of the bunch at the moment of passing the critical energy.

Table 4. Results from numerically modeling the passing of critical energy with a jump, allowing for the effect different impedances have at different intensities

Modeling parameters	95% phase volume	Preservation of the beam (9 GeV)	Features
$\alpha_1 = 0$, simple Without impedance	1.165	100%	Simple model Emittance does not increase
$\alpha_1 = 0$, exact Without impedance	1.167	100%	Exact model Emittance does not increase
$\alpha_1 = 0.01$, exact Without impedance	1.174	100%	No non-linearity Emittance does not increase
$\alpha_1 = 0.01$, exact $Z_n/n = -i10$ 4×10^{11} ppb	1.17	100%	Length shrinks after jump γ_{tr}
$\alpha_1 = 0.01$, exact $Z_n/n = +i10$ 4×10^{11} ppb	1.17	100%	Weak quadrupole oscillations before jump γ_{tr}
$\alpha_1 = 0.01$, exact $Z_n/n = -i10$ 1×10^{12} ppb	1.23	99%	Bunch length shrinks considerably; emittance grows slightly
$\alpha_1 = 0.01$, exact $Z_n/n = +i10$ 1×10^{12} ppb	1.23	99%	High amplitude of quadrupole oscillations; emittance grows slightly

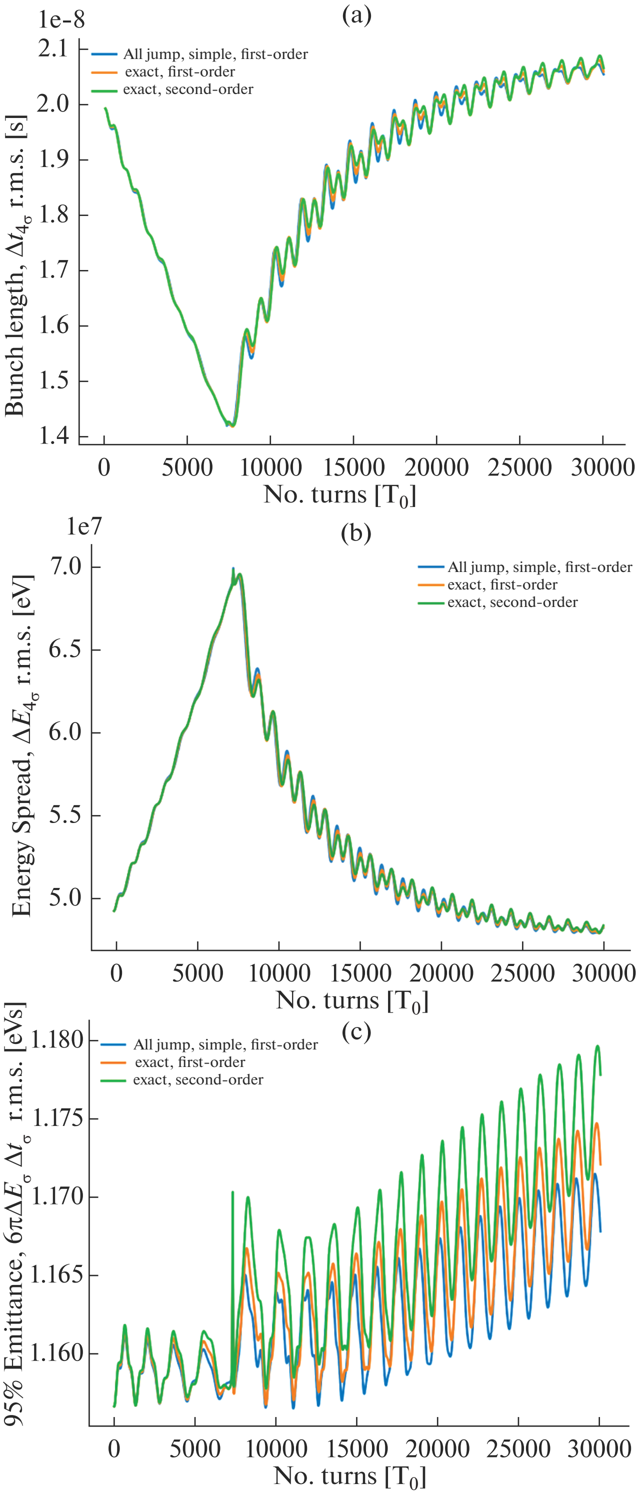

Fig. 8. Dependence of (a) the bunch length, (b) the spread of energy inside the bunch, and (c) the longitudinal emittance on the number of revolutions in the vicinity of the critical energy upon changing the energy from 6.9 to 12.9 GeV for three models with a jump, ignoring the impedance. The blue curve considers only the first order $\eta = \eta_0$ for a simple solver; orange, only the $\eta = \eta_0$ for an exact solver; and green, only $\eta = \eta_0 + \eta_1\delta$.

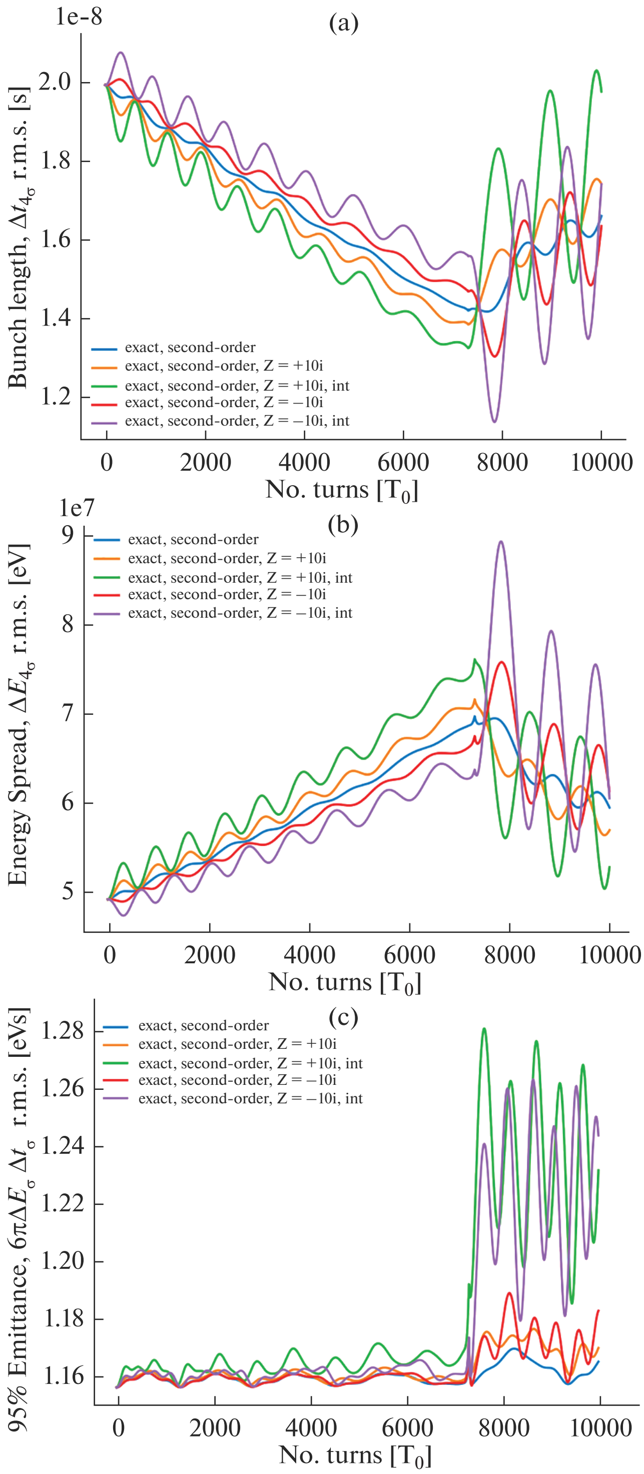

Fig. 9. Dependence of (a) the bunch length, (b) the spread of energy inside the bunch, and (c) the longitudinal emittance on the number of revolutions in the vicinity of the critical energy upon changing the energy from 6.9 to 8.9 GeV with a jump, allowing for different types of impedance and intensities.

The studied dynamics of longitudinal motion near the critical energy is of interest for further study at the NICA complex.

ACKNOWLEDGMENTS

The authors are grateful to S.V. Ivanov, the director of IHEP, for giving us the opportunity to participate in a U-70 synchrotron session; and to IHEP employees V. A. Kalinin, P. T. Pashkov, and A. D. Ermolaev for their comprehensive assistance in our investigation.

FUNDING

This work was supported by ongoing institutional funding. No additional grants to perform or direct this particular research were obtained.

CONFLICT OF INTEREST

The authors of this work declare that they have no conflicts of interest.

REFERENCES

1. W. Hardt, in *Proceedings of the 9th Intenrational Conference on High Energy Acceleration* (Stanford, CA, 1974), p. 434.
2. J. Wei, in *Proceedings of the EPAC92* (1992), Vol. 1, p. 643.
3. P. T. Pashkov, Measuring inductive component of longitudinal coupling impedance in IHEP PS using γ-transition jump, Preprint No. 2004-4, IVFE (Institute for High Energy Physics, Protvino, Moscow oblast, 2004).
4. S. Y. Lee, *Accelerator Physics*, 4th ed. (World Scientific, Singapore, 2018). https://doi.org/10.1142/11111
5. K. Y. Ng, in *Proceedings of the US Particle Accelerator School (USPAS 2002)* (FermiLab, 2002).
6. MADX. https://mad.web.cern.ch/mad/.
7. BLonD. https://blond.web.cern.ch/.
8. P. T. Pashkov, *Fundamentals of Proton Synchrotron Theory: A Textbook for Students of the Lomonosov Moscow State University* (Institut Fiziki Vysokikh Energii, Protvino, Moscow oblast, 1999).
9. S. A. Chernyi, Fiz. Elem. Chastits At. Yadra **22**, 1067 (1991).
10. V. Lebedev, OptiM code. Private communication. www.bdnew.fnal.gov/pba/organizationalchart/lebedev/OptiM/optim.htm.

SPELL OK